3

MICRO- AND NANOENGINEERING APPROACHES TO DEVELOPING GRADIENT BIOMATERIALS SUITABLE FOR INTERFACE TISSUE ENGINEERING

SERGE OSTROVIDOV,[1] AZADEH SEIDI,[2] SAMAD AHADIAN,[1] MURUGAN RAMALINGAM,[1,3,4] AND ALI KHADEMHOSSEINI[1,5,6]

[1] *WPI-Advanced Institute for Materials Research (WPI-AIMR), Tohoku University, Sendai, Japan*

[2] *Technology Center, Okinawa Institute of Science and Technology, Onna-son, Okinawa, Japan*

[3] *Institut National de la Santé Et de la Recherche Médicale UMR977, Faculté de Chirurgie Dentaire, Université de Strasbourg, Strasbourg, France*

[4] *Centre for Stem Cell Research (CSCR), (A unit of Institute for Stem Cell Biology and Regenerative Medicine, Bengaluru) Christian Medical College Campus, Vellore, India*

[5] *Center for Biomedical Engineering, Department of Medicine, Brigham and Women's Hospital, Harvard Medical School, Cambridge, MA, USA*

[6] *Harvard-MIT Division of Health Sciences and Technology, Massachusetts Institute of Technology, Cambridge, MA, USA*

3.1 INTRODUCTION

Interface tissue engineering (ITE) is a rapidly developing field that focuses on the fabrication and development of interfacial tissues for regenerative applications. Interfacial tissues in the human body are primarily found at the interface between

Micro and Nanotechnologies in Engineering Stem Cells and Tissues, First Edition. Edited by Murugan Ramalingam, Esmaiel Jabbari, Seeram Ramakrishna, and Ali Khademhosseini.

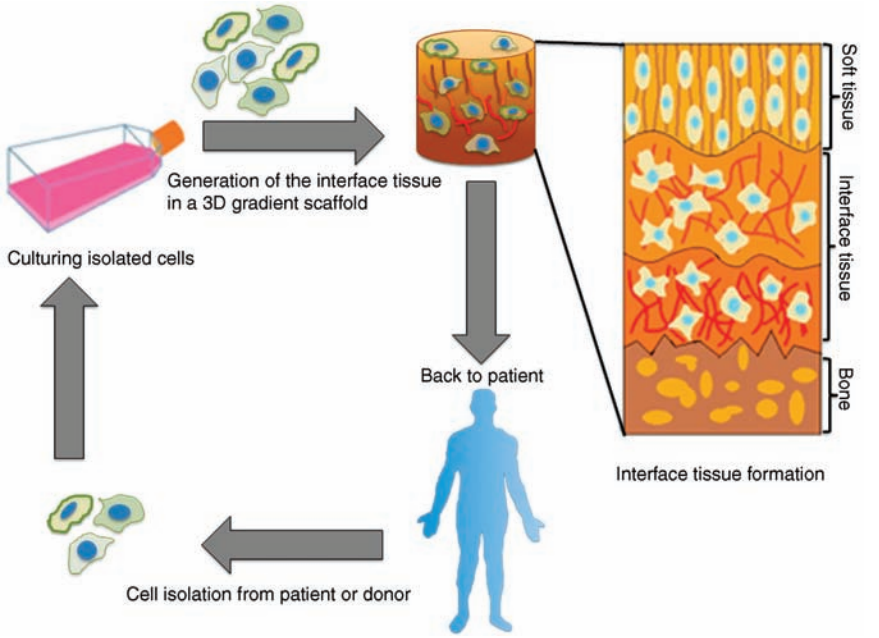

FIGURE 3.1 The concept of interface tissue engineering. 3D = three-dimensional. Modified from Ref. [1] with permission from Elsevier.

soft and hard tissue regions, such as cartilage-to-bone, tendon-to-bone, ligament-to-bone, and other tissue interfaces (e.g., dentin-to-enamel). Tissue engineering (TE) often uses conventional biomaterials to engineer homotypic tissues such as skin, nerve, cartilage, and bone. However, interface tissues are specialized tissues that consist of complex structures with anisotropic properties; thus, conventional biomaterials made of either monophasic or composite materials are inefficient in facilitating interface tissue formation. To engineer an interfacial tissue, biomaterials with a precise distribution of spatial and temporal properties, heterotypic cells, and signaling molecules are required. Therefore, gradient biomaterials with anisotropic properties are more appropriate for ITE studies than their conventional counterparts and may provide a better cellular microenvironment for the support and culture of heterotypic cell populations to generate functional tissue interfaces. A typical ITE process involving gradient biomaterials is schematically illustrated in Figure 3.1.

The development of gradient biomaterials is one of the main criteria for successful ITE development. These gradient biomaterials serve as the extracellular matrix (ECM), providing cells with a temporary structural support to grow and organize into functional tissues.[1] Indeed, the native ECM within tissue interface regions is composed of several biophysical and biochemical cues, which often exist along spatial and temporal gradients. These cues regulate most cell behaviors, such as alignment, motility, differentiation, and mitosis, which assist critical biological processes such as the immune response, embryogenesis, and interface tissue formation. Therefore, synthetic scaffolds made of gradient biomaterials have numerous

advantages over their conventional monophasic counterparts in the context of the material's structure and function for the purpose of interface tissue regeneration. However, the preparation and characterization of gradient biomaterials are generally more difficult than those of homogenous biomaterials because of their complex arrangement and design. Recent advances in micro- and nanoengineering approaches have enabled the development of biomaterials or synthetic scaffolding systems with gradients in material properties that favor the culture and growth of heterotypic cells, particularly with regard to cell differentiation, which is a necessary step toward the development of tissues suitable for ITE.

With these previous findings as a foundation, this chapter discusses various techniques used in the fabrication of gradient biomaterials or scaffolds suitable for engineering tissue interfaces and how the gradient features of the biomaterials influence cellular behaviors such as adhesion, migration, differentiation, and heterotypic interactions during tissue organization. In addition, an overview of various gradient biomaterials and their physical, chemical, and biological classifications is provided. Finally, potential challenges and future directions of the emerging field of ITE are discussed.

3.2 CLASSIFICATION OF GRADIENT BIOMATERIALS

Gradient biomaterials are those with anisotropic properties. Such anisotropies can be observed in the material composition (e.g., different polymer concentrations or compositions), the material structures (e.g., gradients of thickness or porosity), the physical and mechanical properties of the material (e.g., gradients of wettability or stiffness), and the interactions of the material with cells (e.g., cross-gradients of adhesive and nonadhesive polymers). In addition, anisotropies can be added to the material by coating (e.g., gradients of adhesion peptides) or by incorporating a soluble or immobilized molecular factor or drug into the biomaterial.[2] Figure 3.2 presents examples of different types of gradients created in the composition and structure of materials, including gradients in chemical composition, thickness, and porosity.

Gradient biomaterials have recently been used in the field of tissue engineering, and their development for biomedical applications has just begun. Table 3.1 summarizes some gradient types investigated in cell studies. Gradient biomaterials can be generally classified into three types depending on their physical, chemical, and biological properties, which are further discussed below.

3.2.1 Physical Gradients

Biomaterials with physical gradients are referred to as materials with a graded variation in their physical properties, including porosity, stiffness, and topography. Physical gradients are ubiquitous in the human body. Notable examples include bone structure and soft-to-hard interface tissues, such as ligament-to-bone, cartilage-to-bone, or tendon-to-bone interfaces. These interfaces convert the mechanical properties of one tissue into the mechanical properties of the other tissue via a gradual

TABLE 3.1 Gradient Types Used in Cell Studies and Tissue Engineering

Gradients	Materials Used	Applications	References
Physical			
Porosity	Agarose/gelatin gel, polyacrylamide gel	Electrophoresis, bone tissue engineering	[3,4]
Mechanical properties	PLGA nanofiber, agarose gel, polyacrylamide gel	Cell migration, differentiation, tendon-to-bone ITE	[5,6]
Chemical			
Composition	PLGA nanofiber/ hydroxyapatite (HA), collagen/HA	Scaffolds with a gradient of mineralization for ITE	[5,7]
Biological			
Soluble molecules	Poly(2-hydroxyethyl methacrylate) (p(HEMA) gel, polyacrylamide-based gel	Cell attachment and migration; cell proliferation and differentiation; tissue engineering, axonal guidance	[8]
Immobilized molecules	Polyethylene glycol (PEG) gel, agarose gel	Cell adhesion and alignment; cell migration, neurite outgrowth, tissue engineering	[9,10]

ITE = interface tissue engineering.
Modified from Ref. [1] with permission from Elsevier.

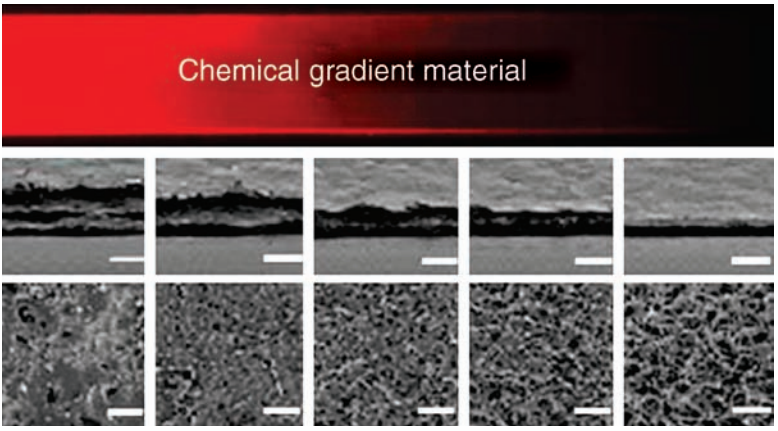

FIGURE 3.2 Poly(ethylene glycol)–diacrylate hydrogel in a microchannel with a chemical composition gradient and its correlated thickness and porosity (scale bar: 50 μm). Adapted from Ref. [1] with permission from John Wiley & Sons.

change in the structural organization and nature of the tissue. Interfacial tissues are complex structures with heterotypic cells surrounded by subtle variations in the ECM, which contains physical, chemical, and mechanical cues. Therefore, scaffolds with graded physical properties are better suited to promoting interface reconstruction.

In tissue engineering, the most frequently used physical gradients are porosity gradients, stiffness gradients, and surface gradients. Porous scaffolds fabricated from biomaterials have also been widely used in tissue reconstruction. In fact, scaffolds with appropriate porosities and interconnected pores with different size ranges are typically required to facilitate cell infiltration and other essential cellular functions. A good example of a physical porosity gradient in the native body is the interface between the cortical and trabecular bone regions, which exhibits a smooth and continuous transition from low porosity at the cortical bone region to high porosity at the trabecular bone region.[11] Porosity and pore size are very important features of a tissue scaffold that greatly affect cell behaviors, particularly cell adhesion, migration, proliferation, and phenotype expression.[12] For example, whereas endothelial cells showed the highest proliferation and ECM production profiles when cultured on scaffolds with a 5 μm pore size compared with scaffolds with larger pore sizes, hepatocytes preferred 20 μm, fibroblasts 90–360 μm, and osteoblasts 100–350 μm pore sizes.[13,14] Consequently, when cells are cultured on a scaffold that has a gradient of porosity or pore size, they tend to preferentially colonize in some areas rather than others. For example, cells from a mixture of chondrocytes, osteoblasts, and fibroblasts cultured on a pore-size gradient colonized in different areas depending on the size of the pores.[15] Chondrocytes and osteoblasts grew well on the larger pore size area, whereas fibroblasts preferred the smaller pore size area. Woodfield et al. showed that a pore size gradient from 200 to 1650 μm promoted an anisotropic bovine chondrocyte cell distribution and anisotropic glycosaminoglycan (GAG) deposition.[16] This anisotropic cell distribution caused by a gradient in porosity or pore size can be used to investigate the interactions of the cells with the scaffold, control cell migration and proliferation, guide tissue ingrowth, or mimic a physiological interface.

Biomaterials with gradients in mechanical properties are often used to engineer interfacial tissues. A good example of a biomechanical gradient in the body is the tendon-to-bone interface, where the stiffness of the bone gradually converts to the elasticity of the ligament.[17,18] In tissue engineering, it is important that a scaffold matches the mechanical properties of the host tissue. For example, in bone regeneration, if the scaffold has lower mechanical properties than the bone itself, the scaffold will not be able to withstand the physiological load and may break. In contrast, if the scaffold has higher mechanical properties than the bone, it will shield the bone from the load and thus may cause bone resorption (stress-shielding effect). A great deal of research is underway to mimic the mechanical properties of bone using gradient biomaterials.

Material stiffness is another key property that affects cell behaviors, notably cell spreading, proliferation, and differentiation. This importance of stiffness exists because cells can precisely sense physical stress and adjust the rigidity of their

cytoskeleton, as their traction force at their anchoring site.[19,20] For example, Kloxin et al. reported the effect of poly(ethylene glycol) (PEG) films on valvular interstitial cells (VICs) with a gradient of elastic modulus ranging from 7 to 32 kPa.[21] These authors observed a graded differentiation of VICs into myofibroblasts, which increased with an increase in the elastic modulus. Decreasing the elastic modulus to 7 kPa led to a reversal of differentiation from myofibroblasts to VICs. Other studies have demonstrated that fibroblasts or smooth muscle cells migrate from softer areas to stiffer areas when cultured on a stiffness gradient.[22] Each cell type responds to stiffness in a different fashion. For example, fibroblasts grow well on stiff materials with a Young's modulus of 34 kPa; neurons prefer soft materials with a Young's modulus of 50 Pa; and smooth muscle cells grow better on materials of moderate stiffness, with a Young's modulus of 8–10 kPa.[23,24] These experimental data show that cells respond strongly to biomaterials with physical gradients.

The surface properties of biomaterials also greatly affect cell behaviors. Surface gradients in terms of roughness, hydrophilicity, and crystallinity have a strong effect on cellular adhesion, spreading, proliferation, and ECM deposition. Washburn et al. introduced a roughness gradient from 0.5 to 13 nm on a poly(L-lactic acid) film and studied the effect of surface roughness with preosteoblastic MC3T3-E1 cells.[25] This study demonstrated that cells responded to roughness and that the cell density decreased with increasing roughness. To investigate the effect of surface features on cellular functions, Meredith et al. used combinatorial methods.[26] These authors fabricated poly(D,L-lactide) (PD)/poly(ε-caprolactone) (PCL) blend libraries with gradients in composition, annealing temperature, and surface structure and loaded them with MC3T3-E1 cells to probe the effects of different surface properties on the cell responses. The experimental data from various studies demonstrate that the cells are highly sensitive to surface features, which dramatically affect cell functionality, shape, size, and regulatory pathways. Therefore, the physical properties of biomaterials must be taken into consideration when designing biomimetic gradient biomaterials for tissue engineering and other biomedical applications.

3.2.2 Chemical Gradients

Biomaterials with chemical gradients are referred here to as materials with gradients of chemical functionalities or properties. This type of gradient biomaterial can be obtained by changing the chemical functionality of the substrate by physical adsorption or chemical bonding. For example, the chemical functionalities of a biomaterial can be changed by treating its surface with plasma or by grafting with chemical functional groups.[27,28] Chemical gradients can also be observed in terms of the material composition of a biomaterial. For example, hydrogels can be polymerized with different material compositions by establishing a prepolymer concentration gradient before cross-linking or by varying the amount of ultraviolet (UV) irradiation during cross-linking.[29] Burdick et al. generated a hydrogel with a gradient of cross-linking densities by using two different poly(ethylene glycol)–diacrylate macromers (10 wt% PEG4000DA and 50 wt% PEG1000DA).[30] After photopolymerization, the 10 wt% macromer solution produced a thin network with a large mesh, whereas the

50 wt% macromer solution produced a larger network with a thin mesh, and the hydrogel presented a thickness gradient from 10 to 50 μm. This alteration results in a hydrogel biomaterial with a gradient in material composition.

The surface chemistry of biomaterials can also be covalently modified by spacers or other functional groups. A classical example is the use of self-assembled monolayers (SAMs). Liu et al. formed a gradient of $C_{11}OH$ SAMs on a gold layer substrate using electrochemical desorption, backfilled the spaces with $C_{15}COOH$, and then activated the carboxyl groups to fix adhesive protein molecules such as fibronectin (FN) or growth factors such as vascular endothelial cell growth factor (VEGF).[31] The cells moved faster toward the protein gradient when the graded surfaces were loaded with bovine aortic endothelial cells (BAECs) compared with the uniform control surface, and the effects of multiple gradients were cumulative. Surface changes have also been applied to obtain a gradient of wettability. For example, Yu et al. generated a gradient from superhydrophobicity to superhydrophilicity on rough gold surfaces via SAM formation.[32] Many of these studies with wettability gradients have focused on cell adhesion and spreading.[33,34] In some cases, a spacer has been used between the substrate and the active molecules or proteins that form the gradient. Mougin et al. generated a PEG gradient by diffusing a PEG–NHS solution through a gel layer coating a cystamine-modified gold surface.[35] When used in cell culture with bovine arteriole endothelium cells (BAVEC-1), a gradient of cell density was observed in the opposite direction of the increasing PEG concentration. These experimental data and others highlight the efficacy of biomaterials with chemical gradients in cell engineering.

3.2.3 Biological Gradients

Biomaterials with biological gradients have gradients of biological moieties such as proteins or biological molecules. Such gradients have been generated using immobilized or soluble forms. Examples include the generation of gradients with adhesive peptides and natural ECM proteins to study the cellular functions and improve biomaterial properties. The cellular response to a concentration gradient has been shown to be much stronger than the response to a single homogenous concentration exposure.[36] Moreover, Wang et al. have shown with human mesenchymal stem cells (hMSCs) that the cellular response can differ along a concentration gradient, as evidenced by the differentiation of stem cells into osteogenic and chondrogenic lineages along a bone morphogenic protein-2 (rhBMP-2) concentration gradient.[37] Different approaches can be used to expose cells to biological gradients.[38] For example, a biological moiety can be grafted onto the surface of a substrate or immobilized in a polymer matrix[9,39,40] or included as a soluble factor in the polymer matrix.[8,41] Similarly, cells can be encapsulated with the gradient in the polymer matrix[42] or attached to the substrate surface.[39] The arginine–glycine–aspartic acid (RGD) motif is a sequence found in native ECM proteins, such as fibronectin, fibrinogen, and laminin, that acts as a cell-adhesion ligand with integrins. RGD is often used to enable cell attachment to polymers such as PEG, which repel cells. NIH3T3 fibroblasts cultured on a PEG hydrogel with an immobilized RGD gradient

aligned and moved along the gradient.[5] In an interesting study, DeLong et al. cultured vascular smooth muscle cells (SMCs) on a gradient of basic fibroblast growth factor (bFGF) immobilized on a PEG substrate with RGD adhesion sites and showed cell migration along the gradient.[10] Jiang et al. have proposed a general method for immobilizing biomolecular gradients on a surface through the use of avidin–biotin bonding.[43] These researchers first immobilized a gradient of avidin on a surface by adsorption and then added a biotinylated molecule of interest. Knapp et al. used a chamber filled with collagen or fibrin gel that was divided into two parts by a Teflon barrier.[44]Human foreskin fibroblast (HFF) cells were encapsulated in one gel part; the other part contained the soluble fibronectin peptide Gly-Arg-Gly-Asp-Ser-Pro (GRGDSP), which is a fibroblast chemotactic factor. When the Teflon barrier was removed, the peptide diffused into the second gel part, forming a gradient of GRGDSP that induced the alignment and migration of the fibroblasts toward the region of higher peptide concentration. Other examples of morphogen gradients include those related to angiogenesis and axonal growth. PC12 neurites were promoted and guided when cultured in a nerve growth factor (NGF) gradient immobilized on poly(2-hydroxyethyl methacrylate) (p(HEMA)) or when cultured in a p(HEMA)/poly-L-lysine (PLL) scaffold loaded with NGF and neurotrophin-3 (NT-3) concentration gradients.[45,46] Similarly, primary fetal neural stem cells (NSCs) showed a rapid induction of glial fibrillary acidic protein (GFAP) when cultured on a hydrogel with a ciliary neurotrophic factor (CNTF) gradient.[47] In the same context, endothelial cells migrated along a surface density gradient of VEGF and formed sprouting elements when exposed to a VEGF gradient in a collagen gel.[31,48] Biological gradients have also been used to study cell metastasis in cancer.[49] Another dynamic research area involving morphogen gradients focuses on bone and cartilage engineering. He et al. have shown that RGD and BMP peptides found in bone morphogenetic protein-2 (BMP-2) acted synergistically when grafted onto a hydrogel to induce bone marrow stromal (BMS) cell osteogenesis and mineralization.[50] Cooper et al. printed a BMP-2 gradient on a DermaMatrix scaffold to demonstrate the spatial control of osteoblast differentiation.[51] Dormer et al. used poly(lactic-*co*-glycolic acid) (PLGA) microspheres loaded with BMP-2 or transforming growth factor beta-1 (TGFβ1) to generate a three-dimensional (3D) scaffold with cross-gradients of those biomolecules.[52] When loaded with human umbilical cord mesenchymal stromal cells (hUCMSCs) or human bone marrow stromal cells (hBMSCs), these gradient scaffolds exhibited spatial and temporal control of the protein release with ECM formation, glycosaminoglycan production, or alkaline phosphatase activity along the increasing concentration gradient. These and other experimental studies have demonstrated that the influence of biological gradients regulates cell behavior.

3.3 MICRO- AND NANOENGINEERING TECHNIQUES FOR FABRICATING GRADIENT BIOMATERIALS

An ideal tissue engineering scaffold should mimic the structure and function of native ECM, in which cells and tissue are organized into 3D architectures and are

triggered by a variety of signaling cues to support cell adhesion, proliferation, and differentiation. Numerous techniques have been used to fabricate materials that are suitable as tissue scaffolds. The next sections discuss the micro- and nanotechnologies that are widely used to fabricate gradient biomaterials.

3.3.1 Salt Leaching

Salt leaching is a popular technique that has been widely used to build scaffolds for tissue engineering, in which salt is used to create the pores or channels in the 3D polymeric scaffolds.[53] This technique involves finely crushing a salt and screening the particles of the desired size followed by casting the mixture of the polymer, salt, and organic solvent into a mold. After solvent evaporation, the salt particles are leached away with water to generate a porous scaffold. Salt leaching is a simple technique for fabricating porous polymeric scaffolds with controlled porosity and pore sizes, which can be achieved by controlling the amount of salt added and the size of the salt particles, respectively. This technique enables the building of materials with a high porosity, up to 92–98%, and with pore sizes ranging from 100 to 700 μm.[54,55] 3D porous scaffolds are used in tissue engineering to support cell attachment, proliferation, infiltration, nutrient transport, and waste removal.[56] However, to build a tissue, the choice of porosity and pore size depends on the cell-type chosen for a specific tissue application. For example, a 5 μm pore size appears optimized for neovascularization, 5–15 μm for fibroblast growth, 20 μm for hepatocytes, 20–125 μm for skin regeneration, 70–120 μm for chondrocytes, 45–150 μm for liver tissue growth, 60–150 μm for vascular smooth muscle adhesion, 100–300 μm for bladder smooth muscle cells, 100–400 μm for bone tissue growth, and 200–350 μm for osteoconduction.[57,58] Therefore, controlling the porosity, pore size, and pore morphology by the porogen[59] is important for the characteristics of a tissue scaffold. At low porosity, with a porogen volume of 65% or less, the number of contact points between particles decreases, leading to incomplete pore interconnectivity and porogen entrapment inside the scaffold.[60] Depending on the porosity and the nature of the porogen, the removal of porogen from the scaffold can be difficult, in which case only a thin scaffold of approximately 4 mm can be prepared. Gradients have been generated directly by salt leaching through pore distribution or pore size or indirectly by surface modification of the porous scaffold. Wu et al. developed a poly(L-lactic acid) (PLLA) scaffold by NaCl particle leaching.[61] The scaffold was placed vertically in a beaker and then aminolyzed along a gradient by wetting it at a controlled speed from bottom to top with a 1,6-hexanediamine–propanol solution. Gelatin was then immobilized by the amino groups via a glutaraldehyde coupling agent to form a gelatin gradient. Another example is a study by Orsi et al., who built gene-activated PEG scaffolds with two different pore size gradients using a gelatin particle template followed by DNA complex adsorption after gel photopolymerization and gelatin leaching.[62] One scaffold type showed a stepwise pore size gradient with 75–150 μm and 300–500 μm pore areas; the second type showed a continuous pore size gradient from 75 to 300 μm. The scaffolds were then loaded with NIH3T3 mouse embryo fibroblasts, and the culture was continued for 16 days. The results

showed that the cells did not penetrate the scaffold at the smallest pore size area, they slowly penetrated the scaffold in the 75–150 μm pore area, and they totally colonized the scaffold in the 150–300 μm and 300–500 μm pore areas. These studies demonstrated the importance of the pore sizes of gradient biomaterials.

3.3.2 Gas Foaming

In gas foaming, a polymer phase is saturated with a gas such as carbon dioxide at high pressure (800 psi). When the pressure inside the chamber is quickly released, gas bubbles are generated and grow in the polymer, a process called "foaming." Upon the completion of the foaming process, the polymeric scaffold turns into a 3D porous structure with an expanded polymeric volume and decreased polymeric density. The amount of dissolved carbon dioxide in the polymer solution determines the porosity and porous structure of the scaffolds. This process produces a sponge-like structure. A technical variation is the use of a chemical reaction with a gas foaming/blowing agent, such as ammonium or sodium bicarbonate, rather than a gas flow.[63] This technique allows for the pore size to range from 100 to 500 μm in the polymer and produces a good porosity, ranging from 60% to 97%, but has low pore interconnectivity and incomplete pore opening because of the formation of a closed external skin during the process.[55,64] To overcome these problems, gas foaming is often combined with microparticulate, salt leaching, or continuous templating techniques.[65–67] Researchers have shown that the microparticle–polymer ratio and particle size control the foam porosity and pore size. By combining gas foaming and sodium chloride microparticulate templating, Salerno et al. showed that increasing the sodium chloride concentration in the PCL polymer matrix from 30 to 80 wt% decreases the pore size in the foam from 71 to 10 μm.[68] These authors used this approach to control pore size and porosity through porogen salt concentration to build a graded scaffold by loading a PCL polymer phase with a sodium chloride concentration gradient from 30 to 60 wt%. They obtained a scaffold with a spatial porosity gradient decreasing from 91% to 83% and a pore size gradient decreasing from 71 to 24 μm. Different fillers, such as hydroxyapatite, β-tricalcium phosphate (β-TCP), carbon fibers, or glass fibers, can also be added to the polymer matrix to change the mechanical properties or bioactivity of the foams.[69] For example, Buhler et al. developed polylactic acid (PLA)-reinforced glass fiber composite graded scaffolds with a volume fiber gradient increasing from 0% in the middle of the scaffold to 10% at the borders and a porosity gradient decreasing from 85% in the center to 65% in the outer zones with an improved flexural modulus.[70] Numerous reports have demonstrated the efficacy of tissue scaffolds prepared by the gas-foaming method.

3.3.3 Phase Separation

In phase separation, a homogenous polymer solution demixes into a polymer-lean phase and a polymer-rich phase due to the addition of an immiscible solvent or to a decrease of the temperature below the solvent melting point. Subsequent freeze-drying of the liquid–liquid phase results in solvent removal and produces

microporous structures. Typically, this technique allows for the formation of micropores (1–10 μm), but it can also be used to generate macropores and to obtain a scaffold with a uniform pore size distribution and good interconnectivity and porosity (>90%).[71] Phase separation can easily be combined with other fabrication technologies (e.g., particulate leaching) to design 3D structures with controlled pore morphology. Although this technique has been effectively used by itself or in combination with other techniques to build tissue scaffolds, very few papers discuss constructing a gradient with phase separation. By combining phase separation and freeze-drying, Van Vlierberghe et al. built a gelatin hydrogel with a pore size gradient decreasing from 330 to 20 μm diameter and porosity gradients decreasing from 82% to 61% porosity.[72] These experimental data and others suggest the potential for the development of tissue engineering scaffolds using phase separation techniques.

3.3.4 Emulsification

In emulsification, a polymer is dissolved in an organic solvent followed by water addition, and the two phases are stirred to obtain an emulsion. The emulsion is then cast and quickly frozen by immersion into nitrogen liquid followed by freeze-drying to remove the dispersed water and solvent, giving to the scaffold a porous structure. Microgels can be constructed by using emulsification in another way. The purpose here is not to generate pores by removing aqueous droplets from a matrix but rather to generate microgel beads by removing the matrix or organic phase after cross-linking.[73,74] However, freeze-drying or lyophilization by itself is a commonly used technique for the fabrication of porous scaffolds, notably collagen sponges, by applying a temperature gradient during the freezing process. This type of scaffolding system has been used in tissue engineering. For example, Harley et al. designed a tubular scaffold with a radial pore size gradient by spinning the polymer solution during the freeze-drying process for a peripheral nerve regeneration application.[75] Near the lumen, the mean pore size was approximately 20 μm, allowing cell penetration from the lumen, whereas near the outer scaffold surface, the mean pore size was 5 μm, impairing cell penetration from the outside. Oh et al. built a PCL scaffold with a pore size gradient by centrifugation of fibril-like PCL in a cylindrical mold and gradually increasing the spinning speed.[15] This processing step was followed by a freeze-drying step and then by a heat fibril-bonding treatment. From top to bottom, the scaffolds obtained by this method had a porosity gradient decreasing from 94% to 80% and a pore size gradient decreasing from 405 to 88 μm. The scaffold's mechanical strength decreases with increasing porosity along the gradient axis. When this scaffold was loaded with a mixture of chondrocytes, osteoblasts, and fibroblast cells and cultured for more than 14 days, chondrocytes and osteoblasts grew well on the larger pore size regions (310–405 μm), whereas fibroblasts preferred to grow in the smaller pore size region (186–200 μm). The efficacy of this type of porous scaffold has also been demonstrated *in vivo*. The scaffolds were implanted without cells into rabbit skull defects, and new bone growth was noted in the region with a pore size of 290–405 μm. Therefore, emulsification-derived scaffolds also play an important role in tissue engineering.

3.3.5 Solid Free-Form Technology

Solid free-form technology (SFF) fabrication encompasses several techniques to manufacture solid structures by delivering energy or materials to specific points in space to produce the structure.[76] Some of these techniques include electron beam melting (EBM), fused deposition modeling (FDM), stereolithography (SLA), laminated object modeling, selective laser sintering (SLS), and 3D printing (3DP). For example, Roy et al. fabricated PLGA scaffolds containing 20 wt% β-tricalcium phosphate with a porosity gradient from 80% to 88% and with pore sizes ranging from 125 to 150 μm by 3DP.[77] Scaffolds implanted into 8 mm-diameter defects in rabbit calvaria showed a new bone density gradient matching the porosity gradient at 8 weeks after surgery. Kalita et al. built TCP–polypropylene (PP) composite scaffolds with a porosity gradient via FDM. Scaffold design was conducted on a computer using CAD software, and the TCP–PP filament was then weaved with different mesh sizes to obtain areas with different pore sizes.[78] In the same context, Lian et al. presented a computer model that reciprocally converts a 3D structure into two-dimensional (2D) stacking concentric patterns.[79] They then used this software to construct an epoxy resin mold via stereolithography and casted calcium phosphate cement (CPC) scaffolds. The software allows for the production of scaffolds with porosity gradients. Thus, SFF is a technique that can be used to fabricate tissue scaffolds with accurate designs or structures that match to specific tissue or organ defects.

3.3.6 Photolithography

Photolithography is a microfabrication technique that allows for the formation of distinct patterns with the desired geometry onto a biomaterial substrate that is suitable for cell studies. During this process, a photoresist polymer undergoes selective photopolymerization caused by selective UV irradiation through a photomask with the desired pattern geometry. Some of the early studies in the use of microfabricated structures and cells were conducted using this approach. For example, in the 1980s, Kleinfield et al. cultured neurons onto photolithographically patterned SAMs.[80] In general, although the pattern resolution obtained by this method is a few micrometers, a high resolution below 100 nm can be achieved using advanced techniques and materials.[81] This technique has many variations and potential applications, but it cannot be used to pattern molecules or biological materials that are UV sensitive. Surfaces patterned by photolithography can be used directly or as templates to generate other patterned surfaces. These surfaces then allow for precise cell manipulation and localization, which facilitates control of cell–cell and cell–material interactions. Although photolithography is basically a 2D process, it is possible to generate 3D structures in a photoresist with gradients in height and/or roughness using gray-scale technology.[82] This technique locally modulates UV exposure doses through a photomask, which has several gray levels, in contrast to conventional binary photomasks that are only black or translucent. Interesting work by Chen et al. showed that a gray photomask can be replaced by microfluidic channel patterns filled with liquids of different color levels and that a

gradient structure can be generated using liquids with decreasing opacity.[83] Thus, Wang et al. used a gray mask technology to generate a protein concentration gradient on an aminated glass coverslip.[84] Using a conventional photomask, Li et al. built a laminin density gradient on a poly(ethylene terephthalate) (PET) substrate by a two-step UV irradiation method.[85] These authors first generated peroxides on the PET surface with a first UV irradiation step and then grafted poly(acrylic acid) (PAA) onto the PET surface with a second UV irradiation step. This process was completed by covalently coupling the amino terminal groups of laminin proteins to the carboxyl groups of PAA. The gradient was generated by moving the substrate below the UV at a controlled speed during the first 3 min of the first UV irradiation, with the result that different areas on the substrate received different amounts of UV and therefore had different amounts of peroxides. When the coverslips were loaded with pheochromocytoma PC12 cells and cultured for 2 days, a cell density gradient matching the laminin density gradient was observed. Toh et al. built a single-density gradient of biotinylated lectin concanavalin A (ConA–biotin) and a double-density gradient of polysaccharide mannan and glycoprotein P-selectin on benzophenone (BP)-coated glass coverslips.[86] The process involved BP-diradical generation via the UV exposure of the substrate through a photomask with a simultaneous flow of biomolecules. BP diradicals then formed covalent bonds with proximal biomolecules. A ConA–biotin gradient was generated by a shutter with a controlled closing speed during UV irradiation, and the double gradients were generated by a controlled rotating shutter. When the resulting materials were loaded with promyelocyte HL-60 cells and cultured for 2 h, a cell density gradient was observed following the P-selectin gradient. When cells in suspension were flowed perpendicularly to the P-selectin gradient, a cell rolling velocity gradient matching the P-selectin gradient was observed. Photolithography can also be used to photopolymerize hydrogels,[87] which could provide a cross-linking density gradient[88] or a patterned gradient with different molecules such as RGD or particles. Based on numerous research studies, photolithography plays an important role in designing scaffold substrates suitable for basic cell studies.

3.3.7 Microfluidics

Microfluidics allows for the patterning of 3D structures suitable for controlling cellular functions. This patterning technique is closely related to microcontact printing. Instead of stamping a polydimethylsiloxane (PDMS) mold with a relief pattern of a master, a microfluidic network is stamped onto a substrate. In this method, the microchannels are used to deliver fluids to selected areas of a substrate, and the substrate is exposed to the flow, resulting in the patterning of the material. This method is frequently used to pattern multiple components on a single substrate and allows for the directed delivery of cells and soluble factors onto the substrate, making it important for applications in cell biology, drug screening, and tissue engineering. Unlike conventional *in vitro* cell culture methods, microfluidics can produce miniature and complex structures mimicking the *in vivo* cellular environment, which is one of the merits of this technique.

From the 1970s to 1990s, microfluidic devices were mainly constructed from silicon and glass substrates using technologies such as photolithography and etching. In the late 1990s, the introduction of soft lithography using polymer materials, in which channels can be molded or embossed rather than etched, allowed for the easier and cheaper fabrication of microfluidic devices. The most widely used polymer to build microfluidic devices for biological applications is PDMS[89–92] because of its material properties, including its biocompatibility, gas permeability, optical transparence down to 280 nm, and ability to replicate microscale features with high fidelity by replica molding. Moreover, PDMS-based soft lithography allows for rapid prototyping. One way to build a gradient with microfluidics is to fill an empty microchannel with capillary force. Density gradients of biomolecules such as proteins can be created in PDMS microchannels because of the adsorption of the biomolecules to the hydrophobic PDMS and because the microfluidic channels have a large surface-area-to-volume ratio, leading to the depletion of the biomolecule from the solution along the channel.[93] The channel outgas technique (COT) involves filling a PDMS microchannel through the inlet reservoir with a biomolecule solution, closing the outlet with a cover glass, and placing the device under vacuum before restoring atmospheric pressure.[94] This technique can produce a gradient from a few hundred micrometers to 1 cm. Another way to build a gradient with microfluidics is to use the diffusion between two liquids. A microchannel is prefilled with solution A, and then solution B is introduced and diffused into the channel.[95] A diffusion gradient with a parabolic shape moves along the channel with the forward flow. If an additional backward flow is generated from the inlet by evaporation, the parabolic profile is flattened, the lateral concentration distribution becomes uniform, and the concentration gradient stabilizes and elongates.[96] This technique can be used to create a centimeter-long gradient. If this backward flow continues, an inverted parabolic profile is formed by the concentration distribution, and the gradient moves backward toward the inlet. To stop this gradient displacement, the backward flow must be prevented by avoiding evaporation. This is done by sealing the inlet, for example by using oil, or by placing the device in a wet atmosphere. He et al. applied this diffusion strategy to build 1–5 cm-long poly(ethylene glycol)–diacrylate (PEG–DA) concentration gradient hydrogels.[39] After freeze-drying, the hydrogel presents a porosity gradient and a decreasing thickness toward low PEG–DA concentrations. Hydrogels were also prepared with the cell-adhesive ligand Arg-Gly-Asp-Ser (RGDS) in a gradient or at a constant concentration. Culturing human umbilical vein endothelial cells (HUVECs) on these hydrogels led to a cell density gradient and a cell morphology gradient (from round shape to well spread) following the RGDS concentration gradient or the PEG–DA concentration gradient when RGDS was constant. A programmed syringe pump can be used to induce repetitive forward and backward flows to lengthen the gradients. For example, Du et al. used alternate forward and backward flows with 30 s intervals between each sequence to allow for lateral mixing by diffusion.[97] Whereas convection stretches the fluid along the channel axis, diffusion acts laterally and tends to suppress hydrodynamic stretching. The use of high-speed (on the order of millimeters per second) flow improves the hydrodynamic stretching and allows for the generation of a long-range gradient of

molecules, microbeads, or cells. Du et al. used this dispersion-based technique to build an HA-gelatin composite hydrogel with a 2–3 cm cross-gradient of hyaluronic acid (HA), which is a cell repellent, and gelatin, which is a bioactive material. SMC cells were cultured for 24 h to study the effect of the cross-gradient, and the cell density gradient followed the gelatin concentration gradient.

Another method of generating gradients is to use laminar flows. Indeed, at a low Reynolds number (<1), no mixing by convection occurs between two adjacent flows, but diffusion is possible. Devices using this technique, such as the T-sensor,[98] involve several separated fluid streams that merge adjacently into a single microchannel. Gradients are generated perpendicular to the flow direction. In 2000, Jeon et al. demonstrated a method for the generation of gradients in chemical composition and surface topography using a microfluidic mixer. This system, built in PDMS, is based on a Christmas tree–shaped microfluidic network, which, from top to bottom, repeatedly splits the streams at the nodes, combines them with neighboring streams, and allows them to mix by diffusion in the serpentine channels.[99] At the end of the network, all streams carrying different concentrations of molecules of interest combine in a broad channel, generating a concentration gradient perpendicular to the flow direction. Using different fluids, a variety of gradients can be generated with a resolution of several microns to several hundred microns. Gradients with different shapes (symmetric or asymmetric), types (smooth, step, multipeaked),[100] and natures (static or dynamic) can also be obtained based on this technique. Using this technique, Burdick et al. built a PEG hydrogel with a gradient of adhesive ligands (RGDS).[30] When HUVECs were cultured on this hydrogel for 3 h, a cell density gradient was observed, matching the RGDS gradient with better spreading toward high RGDS concentrations. These data indicate that microfluidics is a useful technique for building systems that facilitate the studies of cell behavior required for the development of tissue engineering.

3.3.8 Microcontact Printing

Microcontact printing (μCP) is a well-known technique that allows for the transfer of patterns onto biomaterial substrates with high spatial resolution suitable for cell studies. This microfabrication technique is one of the best-known techniques in bioengineering because of its versatility and simplicity for patterning biomaterials without using any expensive equipment. This technique can also be used to pattern a nonplanar surface with a 3D structure when conventional photolithographic techniques would not be feasible. μCP was introduced by the Whitesides group in the early 1990s to replicate patterns generated by photolithography. Initially, this method used the spontaneous adsorption of alkylthiols to form SAMs on gold, which then resist gold etching with alkaline cyanide.[101] μCP was then extended to alkylsiloxanes on silicon oxide, resulting in numerous biological and biotechnological applications.[102,103] Subsequently, other molecular inks[104,105] and other substrates were used, giving rise to numerous variations of μCP.[106] In microcontact printing, a stamp made of a soft polymer, such as polydimethylsiloxane, is soaked in a molecular "ink" that is imprinted on the surface of a substrate.[107,108] The resolution

of the technique is on the order of a few micrometers.[109] However, optimization of the stamp building technique allows for a resolution under 100 nm.[110] Although the μCP technique is simple to use and has several merits, it also has a few drawbacks. For example, stamp swelling during the inking process can result in larger imprinted patterns or resolution problems caused by overdiffusion of the ink; in addition, stamp deformation, such as pairing, buckling, or roof collapse, during contact with the substrate surface results in distorted patterns. μCP has been widely used to modify surfaces, and gradients were built by applying different pressures on the stamp, varying the contact time between the stamp and the substrate, using a nonplanar stamp, gradually soaking the stamp in ink, or gradually depositing the ink on the substrate.[111] Von Philipsborn et al. proposed a protocol to print discontinuous gradients of axon-guidance proteins by a lift-off method or by a casting method.[112] After overnight culture with embryonic chick retinal ganglion cell axons, protein patterns were analyzed for their interactions with axons by fluorescent labeling. Thus, μCP is an important technique that can be used to fabricate bioengineered systems and devices.

3.3.9 Electrospinning

Electrospinning is an easy and versatile technique based on the ejection of a polymeric jet from the tip of an electrically charged syringe, the spinneret, followed by its collection onto a counter electrode, resulting in the formation of fibers with sizes usually ranging from 10 nm to a few micrometers. By manipulating the electrospinning process, the thickness and orientation (aligned or random) of nanofibers can be controlled to match the structure of the targeted tissue.[113] Electrospun fibers have adequate mechanical properties, high porosity, and a large surface-to-volume ratio, which are beneficial properties for interactions with cells and for tissue engineering applications.[114,115] Thus, nanofiber scaffolds have been widely investigated for ligament,[116] meniscus,[117] and bone tissue engineering.[118,119] Nanofiber surfaces can also be modified by bioactive molecules to increase their cellular compatibility.[120,121] One approach to generating a gradient is based on the surface modification of the ejected fibers after electrospinning. Shi et al. incorporated a fibronectin concentration gradient in a polymethylglutarimide (PMGI) electrospun mesh scaffold by wetting the scaffold at a controlled speed from bottom to top with fibronectin solution in a vertical PDMS microchamber.[122,123] Loaded with NIH3T3 cells and cultured for 24 h, the scaffold showed a cell density gradient decreasing from 1400 cells/mm^2 (at the bottom of the scaffold) to 100 cells/mm^2 (at the top of the scaffold), following the fibronectin concentration gradient. To mimic the tendon–bone interface, Li et al. coated the electrospun nanofibers of PLGA and PCL mats with a calcium phosphate mineralization gradient by wetting the scaffolds at a controlled speed from bottom to top with 10-fold concentrated simulated body fluid (10 SBF) solution in a glass.[7] The mineralization gradient decreased from 37.8% (at the scaffold bottom) to 0.7% (at the scaffold top) in calcium phosphate and from 33.9% to 0.8% for the PLGA and PCL scaffolds, respectively. When the PLGA scaffold is subjected to uniaxial tensile deformation, the Young's modulus follows

the mineralization gradient and decreases with the decrease in mineralization. This stiffness gradient induced by the mineralization gradient mimics the stiffness distribution at the tendon–bone interface. In contrast, when the PCL scaffold was loaded with mouse preosteoblast MC3T3-E1 cells and cultured for 3 days, it showed a cell density gradient decreasing from 435 cells/mm^2 (at the bottom of the scaffold) to 115 cells/mm^2 (at the top of the scaffold) following the mineralization gradient, and the cells were oriented toward the higher mineralization area. The same group also fabricated a PLGA electrospun nanofiber scaffold with a random fiber orientation area and an aligned fiber orientation area combined with a calcium phosphate mineralization gradient decreasing from a random to an aligned fiber orientation to mimic both the composition and structure seen at the bone–tendon interface.[124] Recently, coupling microfluidics with the laminar flow of polymers to electrospray and electrospinning techniques, Lahann et al. have obtained multicompartmental spherical particles and aligned biodegradable PLGA multicompartmental microfibers with narrow polydispersity.[125–127] Because microfluidic systems can generate gradients, it is possible to couple a gradient microfluidic generator to the electrospinning setup, which would allow for the direct electrospinning of graded fibers. The experimental data obtained from these and other studies demonstrate that electrospinning can be used to fabricate scaffolds with gradients in physical and chemical properties mimicking the natural ECM at the interface zones.

3.3.10 Nanoimprint Lithography

Nanoimprint lithography (NIL) is a cost-effective and high-throughput technique for fabricating nanopatterns. NIL does not require any expensive instrumentation or sophisticated clean-room facilities, which are required for conventional lithographic techniques such as photolithography; thus, NIL is more suitable for biological applications. Moreover, the repartition of chemical compounds on the structured surface can be controlled. This technique can be applied to create 2D or 3D nanotopographical patterns of different geometry and can be used on a wide range of biomaterial substrates suitable for cell engineering. In NIL,[128] a thermoplastic or UV-curing polymer layer is imprinted by a mold and cured by heat (hot embossing or thermal-NIL) or by UV irradiation (UV-NIL) at the same time. In the latter case, the mold is usually in quartz so that it is permeable to UV. After cooling down or UV curing, the stamp is removed from the imprinted polymer, which contains the reversed stamp topography. This technique allows for a resolution of a few nanometers.[129] Limited data are available on generating gradients by nanoimprinting methods for biological applications. For a DNA stretching application, Cao et al. used nanoimprint lithography to build a structure with a size gradient from the micrometer to nanometer scale to overcome the difficulties of introducing long-genomic DNA molecules into nanometer-scale channels.[130] In two short preliminary reports, Sun et al. built patterns of parallel line and space gratings on polystyrene or dimethylacrylate surfaces with height gradients from 0 to 360 nm using nanoimprinting technology.[131,132] When murine preosteoblast MC3T3-E1 cells were loaded onto these surfaces and cultured for

2 days, a cell alignment and elongation gradient was observed that decreased with the height pattern.

3.3.11 Inkjet Printing

Inkjet printing is a noncontact reprographic method that translates numerical data from a computer into a pattern on a substrate using ink drops.[133] This technology is widely used in the electronics industry to print integrated circuits.[134] In the late 1990s, inkjet printing was adapted to biological applications with the printing of SAMs, DNA arrays, and other proteins.[135,136] Notably, this technology was used to pattern cells by printing ECM molecules.[137] Recently, it has become possible to directly print living cells, opening up an avenue to applications in tissue engineering and organ printing.[138,139] Indeed, it is possible to build a 3D structure by printing superimposed cell layers. Recent works have reported the printing of 3D hydrogels and hydrogels with cells.[140] Inkjet printing allows for high-precision cell positioning with a resolution of approximately 100 μm with a bio-ink and fast prototyping and manufacturing.[141] In color printers, inks can be replaced by different biological components, such as proteins, peptides, growth factors, polymers, drugs, or different cell lines, and all components can be printed simultaneously onto a culture dish, culture sheet, 3D scaffold, gel, or liquid. Because gradients can be easily designed on a computer by continuously fading a color, cell gradient patterns can be built by printing a collagen solution with a decrease in the spatial density of the bio-ink droplets.[137] Another strategy for printing gradients consists of overprinting, in which several bio-ink depositions are performed on the same spot. A density gradient can be obtained by controlling the number of overprints in a spatial repartition. Thus, Campbell et al. printed a fibroblast growth factor-2 (FGF-2) gradient on fibrin film using an overprinting strategy.[142] After 4 days of culturing the film with human MG-63 osteosarcoma cells, the team observed a cell density gradient following the hormonal gradient. Because cells or bacteria can be directly printed, Xu et al. printed bacterial density gradients of *Escherichia coli* on an agarose-coated coverslip by using an *E. coli* suspension as a bio-ink.[143] Ilkhanizadeh et al. printed different protein gradients on Hydrogel-coated slides from Perkin Elmer.[47] These authors showed that a printed gradient of Cy5-conjugated transferrin exhibited good stability in culture medium at 37°C over 22 h, which is enough time to induce a cellular response. In another example, Ilkhanizadeh et al. printed a CNTF gradient on a hydrogel. Because CNTF induced the differentiation of NSCs into astrocytes, which express GFAP, these authors observed a GFAP-positive cell density gradient decreasing from 14% to 6%, reflecting the printed CNTF gradient. NIL is an emerging technique for the development of scaffold systems with various biological applications.

3.3.12 Gradient Makers

The development of gradient makers dates from the 1960s. One interesting idea was presented by Alberto, who adapted a conventional 30 ml syringe to an exponential

gradient maker that can be used to make a gradient material.[144] The syringe outlet is plugged to a tube that is clamped. The syringe body is half filled with solution A with no concentration of the molecule of interest and a stir bar (chamber 1). The syringe plunger is modified by notching the up and down borders of the rubber sealing tip. The notched plunger is pushed into the syringe until no air space remains. Then the upper part of the syringe body is filled with solution B with a high concentration of the molecule of interest (chamber 2). When the outlet is unclamped, solution A begins to flow out, and solution B begins to flow into chamber 1 via the notched rubber and mix with solution A. Current gradient makers[144] are similar, consisting of two chambers, A and B, connected at the bottom by a pipe with a valve. Chamber B is also connected at the bottom to a peristaltic pump by an outlet pipe. Chamber A contains a solution with a high concentration of the molecule of interest, and chamber B contains a solution without or with a low concentration of the molecule of interest and a stir bar. When the valve is opened and the pump is started, the solution from chamber A is drawn into the pipe and mixed completely with the chamber B solution before it is delivered by the outlet pipe. A gradient is formed because the solution from chamber A is mixed with a decreasing volume of solution from chamber B. These types of gradient makers have been proposed by companies such as CBS Scientific, Hoefer, and GE Healthcare. Many studies have used a gradient maker to fabricate gradient biomaterials. For example, Chatterjee et al. used a gradient maker to fabricate a PEG hydrogel with a gradient of PEG concentrations ranging from 5% to 20%, resulting in a gradient of compressive modulus from 10 to 300 kPa. The encapsulation of MC3T3-E1 cells showed that the material property induced a screening of cell differentiation and showed a gradient of mineralization, which revealed that osteoblasts differentiate in the hydrogel region with a modulus of 225 kPa or greater.[145] These data indicate that gradient makers have great potential for designing gradient biomaterials suitable for tissue engineering.

3.4 CONCLUSIONS

Gradient biomaterials are new arrivals to the field of tissue engineering, and their introduction has led to the development of ITE. In contrast to conventional homotypic tissue engineering, ITE requires specially designed biomaterials that can mimic the structure and function of native heterotypic interface tissues, which contain several gradient features. Therefore, the development of biomaterials with gradients in mechanical properties, composition, structure, or incorporated biomolecules is essential. Micro- and nanotechnologies allow for the fabrication of such gradient biomaterials and can be used to create new, advanced gradient biomaterials for ITE applications. This chapter discussed some widely used techniques for the fabrication of gradient biomaterials and considered their merits and shortcomings as well as how the various gradient biomaterials can be used in basic cell studies and tissue engineering. Future developments of gradient biomaterials for ITE applications will include the design of new engineered surfaces and drug-releasing scaffolds, modified with several bioactive molecules, such as growth factors,

enzymes, ECM proteins, and DNA, to facilitate the tissue regeneration process by mimicking the ECM environment. In this regard, the inclusion within the scaffolds of the temporal control of the activity of these bioactive molecules to complement the spatial gradients would be an advantage. Indeed, the native ECM contains a plethora of physical and chemical cues that often exist in gradients and actively and temporally induce cellular responses such as migration and differentiation. Other points to be addressed for the fabrication of biomimetic scaffolds will be to localize the distribution of the physical and chemical properties within the scaffold and to favor the cooperation of heterotypic cells in the scaffold as well as with the surrounding host environment at the insertion sites. This interfacial tissue regeneration should result in the formation of a tissue with gradient properties in terms of cell type and ECM components. Thus, gradient biomaterials hold great promise for the field of ITE.

ACKNOWLEDGMENTS

This work was supported by the World Premier International Research Center Initiative (WPI), MEXT, Japan.

REFERENCES

1. Seidi A, Ramalingam M, Elloumi-Hannachi I, Ostrovidov S, Khademhosseini A. Gradient biomaterials for soft-to-hard interface tissue engineering. Acta Biomater 2011;7(4):1441–1451.
2. Singh M, Berkland C, Detamore MS. Strategies and applications for incorporating physical and chemical signal gradients in tissue engineering. Tissue Eng Part B Rev 2008;14(4):341–366.
3. Tripathi A, Kathuria N, Kumar A. Elastic and macroporous agarose–gelatin cryogels with isotropic and anisotropic porosity for tissue engineering. J Biomed Mater Res Part A 2009;90A(3):680–694.
4. Liu C, Han Z, Czernuszka JT. Gradient collagen/nanohydroxyapatite composite scaffold: development and characterization. Acta Biomater 2009;5(2):661–669.
5. Guarnieri D, Borzacchiello A, De Capua A, Ruvo M, Netti PA. Engineering of covalently immobilized gradients of RGD peptides on hydrogel scaffolds: effect on cell behaviour. Macromol Symp 2008;266(1):36–40.
6. Lo CT, Throckmorton DJ, Singh AK, Herr AE. Photopolymerized diffusion-defined polyacrylamide gradient gels for on-chip protein sizing. Lab Chip 2008;8(8):1273–1279.
7. Li X, Xie J, Lipner J, Yuan X, Thomopoulos S, Xia Y. Nanofiber scaffolds with gradations in mineral content for mimicking the tendon-to-bone insertion site. Nano Lett 2009;9(7):2763–2768.
8. Peret BJ, Murphy WL. Controllable soluble protein concentration gradients in hydrogel networks. Adv Funct Mater 2008;18(21):3410–3417.
9. Cosson S, Kobel SA, Lutolf MP. Capturing complex protein gradients on biomimetic hydrogels for cell-based assays. Adv Funct Mater 2009;19(21):3411–3419.

10. DeLong SA, Moon JJ, West JL. Covalently immobilized gradients of bFGF on hydrogel scaffolds for directed cell migration. Biomaterials 2005;26(16):3227–3234.
11. Hsu Y, Turner I, Miles A. Fabrication of porous bioceramics with porosity gradients similar to the bimodal structure of cortical and cancellous bone. J Mater Sci 2007;18 (12):2251–2256.
12. Miot S, Woodfield T, Daniels AU, Suetterlin R, Peterschmitt I, Heberer M, et al. Effects of scaffold composition and architecture on human nasal chondrocyte redifferentiation and cartilaginous matrix deposition. Biomaterials 2005;26(15):2479–2489.
13. Tanaka M, Takayama A, Ito E, Sunami H, Yamamoto S, Shimomura M. Effect of Pore size of self-organized honeycomb-patterned polymer films on spreading, focal adhesion, proliferation, and function of endothelial cells. J Nanosci Nantechnol 2007;7(3): 763–772.
14. Whang K, Healy KE, Elenz DR, Nam EK, Tsai DC, Thomas CH, et al. Engineering bone regeneration with bioabsorbable scaffolds with novel microarchitecture. Tissue Eng 1999;5(1):35–51.
15. Oh SH, Park IK, Kim JM, Lee JH. *In vitro* and *in vivo* characteristics of PCL scaffolds with pore size gradient fabricated by a centrifugation method. Biomaterials 2007;28 (9):1664–1671.
16. Woodfield TBF, Blitterswijk CAV, Wijn JD, Sims TJ, Hollander AP, Riesle J. Polymer scaffolds fabricated with pore-size gradients as a model for studying the zonal organization within tissue-engineered cartilage constructs. Tissue Eng 2005;11(9–10): 1297–1311.
17. Benjamin M, Toumi H, Ralphs JR, Bydder G, Best TM, Milz S. Where tendons and ligaments meet bone: attachment sites ("entheses") in relation to exercise and/or mechanical load. J Anat 2006;208(4):471–490.
18. Moffat KL, Wang INE, Rodeo SA, Lu HH. Orthopedic interface tissue engineering for the biological fixation of soft tissue grafts. Clin Sports Med 2009;28(1):157–176.
19. Discher DE, Janmey P, Wang Y-l. Tissue cells feel and respond to the stiffness of their substrate. Science 2005;310(5751):1139–1143.
20. Choquet D, Felsenfeld DP, Sheetz MP. Extracellular matrix rigidity causes strengthening of integrin-cytoskeleton linkages. Cell 1997;88(1):39–48.
21. Kloxin AM, Benton JA, Anseth KS. *In situ* elasticity modulation with dynamic substrates to direct cell phenotype. Biomaterials 2010;31(1):1–8.
22. Georges PC, Janmey PA. Cell type-specific response to growth on soft materials. J Appl Physiol 2005;98(4):1547–1553.
23. Gray DS, Tien J, Chen CS. Repositioning of cells by mechanotaxis on surfaces with micropatterned Young's modulus. J Biomed Mater Res Part A 2003;66A(3):605–614.
24. Zaari N, Rajagopalan P, Kim SK, Engler AJ, Wong JY. Photopolymerization in microfluidic gradient generators: microscale control of substrate compliance to manipulate cell response. Adv Mater 2004;16(23–24):2133–2137.
25. Washburn NR, Yamada KM, Simon CG, Jr., Kennedy SB, Amis EJ. High-throughput investigation of osteoblast response to polymer crystallinity: influence of nanometer-scale roughness on proliferation. Biomaterials 2004;25(7–8):1215–1224.
26. Meredith JC, Sormana J-L, Keselowsky BG, García AJ, Tona A, Karim A, et al. Combinatorial characterization of cell interactions with polymer surfaces. J Biomed Mater Res Part A 2003;66A(3):483–490.

27. Barry JJA, Silva MMCG, Shakesheff KM, Howdle SM, Alexander MR. Using Plasma deposits to promote cell population of the porous interior of three-dimensional poly(D,L-lactic acid) tissue-engineering scaffolds. Adv Funct Mater 2005;15(7): 1134–1140.
28. Whittle JD, Barton D, Alexander MR, Short RD. A method for the deposition of controllable chemical gradients. Chem Commun 2003; (14):1766–1767.
29. Johnson PM, Reynolds TB, Stansbury JW, Bowman CN. High throughput kinetic analysis of photopolymer conversion using composition and exposure time gradients. Polymer 2005;46(10):3300–3306.
30. Burdick JA, Khademhosseini A, Langer R. Fabrication of gradient hydrogels using a microfluidics/photopolymerization process. Langmuir 2004;20(13):5153–5156.
31. Liu L, Ratner BD, Sage EH, Jiang S. Endothelial cell migration on surface-density gradients of fibronectin, VEGF, or both proteins. Langmuir 2007;23(22):11168–11173.
32. Yu X, Wang Z, Jiang Y, Zhang X. Surface gradient material: from superhydrophobicity to superhydrophilicity. Langmuir 2006;22(10):4483–4486.
33. Ruardy TG, Schakenraad JM, van der Mei HC, Busscher HJ. Adhesion and spreading of human skin fibroblasts on physicochemically characterized gradient surfaces. J Biomed Mater Res 1995;29(11):1415–1423.
34. Lee JH, Khang G, Lee JW, Lee HB. Interaction of different types of cells on polymer surfaces with wettability gradient. J Colloid Interface Sci 1998;205(2):323–330.
35. Mougin K, Ham AS, Lawrence MB, Fernandez EJ, Hillier AC. Construction of a tethered poly(ethylene glycol) surface gradient for studies of cell adhesion kinetics. Langmuir 2005;21(11):4809–4812.
36. Okuyama T, Yamazoe H, Seto Y, Suzuki H, Fukuda J. Cell micropatterning inside a microchannel and assays under a stable concentration gradient. J Biosci Bioeng 2010;110(2):230–237.
37. Wang X, Wenk E, Zhang X, Meinel L, Vunjak-Novakovic G, Kaplan DL. Growth factor gradients via microsphere delivery in biopolymer scaffolds for osteochondral tissue engineering. J Control Release 2009;134(2):81–90.
38. Sant S, Hancock MJ, Donnelly JP, Iyer D, Khademhosseini A. Biomimetic gradient hydrogels for tissue engineering. Can J Chem Eng 2010;88(6):899–911.
39. He J, Du Y, Villa-Uribe JL, Hwang C, Li D, Khademhosseini A. Rapid generation of biologically relevant hydrogels containing long-range chemical gradients. Adv Funct Mater 2010;20(1):131–137.
40. DeLong SA, Gobin AS, West JL. Covalent immobilization of RGDS on hydrogel surfaces to direct cell alignment and migration. J Control Release 2005;109(1–3): 139–148.
41. Ostrovidov S, Annabi N, Seidi A, Ramalingam M, Dehghani F, Kaji H, et al. Controlled release of drugs from gradient hydrogels for high-throughput analysis of cell-drug interactions. Anal. Chem. 2012, 84, (3), 1302–1309.
42. Phillips JE, Burns KL, Le Doux JM, Guldberg RE, Garcia AJ. Engineering graded tissue interfaces. Proc Nat Acad Sci 2008;105(34):12170–12175.
43. Jiang X, Xu Q, Dertinger SKW, Stroock AD, Fu TM, Whitesides GM. A General method for patterning gradients of biomolecules on surfaces using microfluidic networks. Anal Chem 2005;77(8):2338–2347.

44. Knapp DM, Helou EF, Tranquillo RT. A Fibrin or collagen gel assay for tissue cell chemotaxis: assessment of fibroblast chemotaxis to GRGDSP. Exp Cell Res 1999;247 (2):543–553.
45. Kapur TA, Shoichet MS. Immobilized concentration gradients of nerve growth factor guide neurite outgrowth. J Biomed Mater Res Part A 2004;68A(2):235–243.
46. Moore K, Macsween M, Shoichet M. Immobilized concentration gradients of neurotrophic factors guide neurite outgrowth of primary neurons in macroporous scaffolds. Tissue Eng 2006;12(2):267–278.
47. Ilkhanizadeh S, Teixeira AI, Hermanson O. Inkjet printing of macromolecules on hydrogels to steer neural stem cell differentiation. Biomaterials 2007;28(27): 3936–3943.
48. Chung S, Sudo R, Mack PJ, Wan C-R, Vickerman V, Kamm RD. Cell migration into scaffolds under co-culture conditions in a microfluidic platform. Lab Chip 2009;9 (2):269–275.
49. Torisawa Y-s, Mosadegh B, Bersano-Begey T, Steele JM, Luker KE, Luker GD, et al. Microfluidic platform for chemotaxis in gradients formed by CXCL12 source-sink cells. Integr Biol 2010;2(11–12):680–686.
50. He X, Ma J, Jabbari E. Effect of grafting RGD and BMP-2 protein-derived peptides to a hydrogel substrate on osteogenic differentiation of marrow stromal cells. Langmuir 2008;24(21):12508–12516.
51. Cooper GM, Miller ED, DeCesare GE, Usas A, Lensie EL, Bykowski MR, et al. Inkjet-based biopatterning of bone morphogenetic protein-2 to spatially control calvarial bone formation. Tissue Eng Part A 2010;16(5):1749–1759.
52. Dormer N, Singh M, Wang L, Berkland C, Detamore M. Osteochondral interface tissue engineering using macroscopic gradients of bioactive signals. Ann Biomed Eng 2010;38 (6):2167–2182.
53. Chevalier E, Chulia D, Pouget C, Viana M. Fabrication of porous substrates: a review of processes using pore forming agents in the biomaterial field. J Pharm Sci 2008;97(3): 1135–1154.
54. Nazarov R, Jin H-J, Kaplan DL. Porous 3-D scaffolds from regenerated silk fibroin. Biomacromolecules 2004;5(3):718–726.
55. Reignier J, Huneault MA. Preparation of interconnected poly(ε-caprolactone) porous scaffolds by a combination of polymer and salt particulate leaching. Polymer 2006;47 (13):4703–4717.
56. Karageorgiou V, Kaplan D. Porosity of 3D biomaterial scaffolds and osteogenesis. Biomaterials 2005;26(27):5474–5491.
57. Dietmar WH. Scaffolds in tissue engineering bone and cartilage. Biomaterials 2000;21 (24):2529–2543.
58. Annabi N, et al. Controlling the porosity and microarchitecture of hydrogels for tissue engineering. Tissue Eng 2010;16(4):371.
59. Zhang J, Wu L, Jing D, Ding J. A comparative study of porous scaffolds with cubic and spherical macropores. Polymer 2005;46(13):4979–4985.
60. Hou Q, Grijpma DW, Feijen J. Porous polymeric structures for tissue engineering prepared by a coagulation, compression moulding and salt leaching technique. Biomaterials 2003;24(11):1937–1947.

61. Wu J, Tan H, Li L, Gao C. Covalently immobilized gelatin gradients within three-dimensional porous scaffolds. Chin Sci Bull 2009;54(18):3174–3180.
62. Orsi S, Guarnieri D, Netti P. Design of novel 3D gene activated PEG scaffolds with ordered pore structure. J Mater Sci 2010;21(3):1013–1020.
63. Kim TK, Yoon JJ, Lee DS, Park TG. Gas foamed open porous biodegradable polymeric microspheres. Biomaterials 2006;27(2):152–159.
64. Park CB, Baldwin DF, Suh NP. Effect of the pressure drop rate on cell nucleation in continuous processing of microcellular polymers. Polymer Eng Sci 1995;35(5): 432–440.
65. Lee PC, Wang J, Park CB. Extrusion of microcellular open-cell LDPE-based sheet foams. J Appl Polymer Sci 2006;102(4):3376–3384.
66. Haugen H, Will J, Fuchs W, Wintermantel E. A novel processing method for injection-molded polyether–urethane scaffolds. Part 1: processing. J Biomed Mater Res Part B 2006;77B(1):65–72.
67. Salerno A, Oliviero M, Di Maio E, Iannace S, Netti PA. Design and preparation of μ-bimodal porous scaffold for tissue engineering. J Appl Polymer Sci 2007;106 (5):3335–3342.
68. Salerno A, Iannace S, Netti PA. Open-pore biodegradable foams prepared via gas foaming and microparticulate templating. Macromol Biosci 2008;8(7):655–664.
69. Slivka MA, Leatherbury NC, Kieswetter K, Niederauer GG. Porous, resorbable, fiber-reinforced scaffolds tailored for articular cartilage repair. Tissue Eng 2001;7(6): 767–780.
70. Buhler M, Bourban P-E, Manson J-AE. Cellular thermoplastic composites with micro-structural gradients of fibres and porosity. Composites Sci Technol 2008;68(3–4): 820–828.
71. Nam YS, Park TG. Porous biodegradable polymeric scaffolds prepared by thermally induced phase separation. J Biomed Mater Res 1999;47(1):8–17.
72. Van Vlierberghe S, Cnudde V, Dubruel P, Masschaele B, Cosijns A, De Paepe I, et al. Porous gelatin hydrogels: 1. cryogenic formation and structure analysis. Biomacromolecules 2007;8(2):331–337.
73. Wheeldon I, Ahari AF, Khademhosseini A. Microengineering hydrogels for stem cell bioengineering and tissue regeneration. JALA Charlottesv Va 2010;15(6):440–448.
74. Khademhosseini A, Langer R. Microengineered hydrogels for tissue engineering. Biomaterials 2007;28(34):5087–5092.
75. Harley BA, Hastings AZ, Yannas IV, Sannino A. Fabricating tubular scaffolds with a radial pore size gradient by a spinning technique. Biomaterials 2006;27(6):866–874.
76. Hutmacher DW, Sittinger M, Risbud MV. Scaffold-based tissue engineering: rationale for computer-aided design and solid free-form fabrication systems. Trends Biotechnol 2004;22(7):354–362.
77. Roy TD, Simon JL, Ricci JL, Rekow ED, Thompson VP, ParsonsJr., Performance of degradable composite bone repair products made via three-dimensional fabrication techniques. J Biomed Mater Res Part A 2003;66A(2):283–291.
78. Kalita SJ, Bose S, Hosick HL, Bandyopadhyay A. Development of controlled porosity polymer-ceramic composite scaffolds via fused deposition modeling. Mater Sci Eng C 2003;23(5):611–620.

79. Lian Q, Li D-C, Tang Y-P, Zhang Y-R. Computer modeling approach for a novel internal architecture of artificial bone. Computer-Aided Design 2006;38(5):507–514.
80. Kleinfeld D, Kahler KH, Hockberger PE. Controlled outgrowth of dissociated neurons on patterned substrates. J Neurosci 1988;8(11):4098–4120.
81. Nie Z, Kumacheva E. Patterning surfaces with functional polymers. Nat Mater 2008;7 (4):277–290.
82. Waits CM, Modafe A, Ghodssi R. Investigation of gray-scale technology for large area 3D silicon MEMS structures. J Micromech Microeng 2003;13(2):170.
83. Chen C, Hirdes D, Folch A. Gray-scale photolithography using microfluidic photomasks. Proc Natl Acad Sci 2003;100(4):1499–1504.
84. Wang S, Wong Po Foo C, Warrier A, Poo M-m, Heilshorn S, Zhang X. Gradient lithography of engineered proteins to fabricate 2D and 3D cell culture microenvironments. Biomed Microdevices 2009;11(5):1127–1134.
85. Li B, Ma Y, Wang S, Moran PM. A technique for preparing protein gradients on polymeric surfaces: effects on PC12 pheochromocytoma cells. Biomaterials 2005;26 (13):1487–1495.
86. Toh Y-C, Lim TC, Tai D, Xiao G, van Noort D, Yu H. A microfluidic 3D hepatocyte chip for drug toxicity testing. Lab Chip 2009;9(14):2026–2035.
87. Slaughter BV, Khurshid SS, Fisher OZ, Khademhosseini A, Peppas NA. Hydrogels in regenerative medicine. Adv Mater 2009;21(32–33):3307–3329.
88. Peppas NA, Hilt JZ, Khademhosseini A, Langer R. Hydrogels in biology and medicine: from molecular principles to bionanotechnology. Adv Mater 2006;18(11):1345–1360.
89. Mizuno J, Ostrovidov S, Sakai Y, Fujii T, Nakamura H, Inui H. Human ART on chip: improved human blastocyst development and quality with IVF-chip. Fertil Steril 2007;88:S101.
90. Ostrovidov S, Sakai Y, Fujii T. Integration of a pump and an electrical sensor into a membrane-based PDMS microbioreactor for cell culture and drug testing. Biomed Microdevices 2011;13(5):847–864.
91. Ostrovidov S, Jiang J, Sakai Y, Fujii T. Membrane-based PDMS microbioreactor for perfused 3D primary rat hepatocyte cultures. Biomed Microdevices 2004;6(4): 279–287.
92. McDonald JC, Duffy DC, Anderson JR, Chiu DT, Wu H, Schueller OJA, et al. Fabrication of microfluidic systems in poly(dimethylsiloxane). Electrophoresis 2000;21(1):27–40.
93. Fosser KA, Nuzzo RG. Fabrication of patterned multicomponent protein gradients and gradient arrays using microfluidic depletion. Anal Chem 2003;75(21):5775–5782.
94. Monahan J, Gewirth AA, Nuzzo RG. A method for filling complex polymeric microfluidic devices and arrays. Anal Chem 2001;73(13):3193–3197.
95. Du Y, Shim J, Vidula M, Hancock MJ, Lo E, Chung BG, et al. Rapid generation of spatially and temporally controllable long-range concentration gradients in a microfluidic device. Lab Chip 2009;9(6):761–767.
96. Walker GM, Beebe DJ. An evaporation-based microfluidic sample concentration method. Lab Chip 2002;2(2):57–61.
97. Du Y, Hancock MJ, He J, Villa-Uribe JL, Wang B, Cropek DM, et al. Convection-driven generation of long-range material gradients. Biomaterials 2010;31(9):2686–2694.

98. Kamholz AE, Weigl BH, Finlayson BA, Yager P. Quantitative analysis of molecular interaction in a microfluidic channel: the T-sensor. Anal Chem 1999;71(23):5340–5347.
99. Jeon NL, Dertinger SKW, Chiu DT, Choi IS, Stroock AD, Whitesides GM. Generation of solution and surface gradients using microfluidic systems. Langmuir 2000;16(22): 8311–8316.
100. Dertinger SKW, Chiu DT, Jeon NL, Whitesides GM. Generation of gradients having complex shapes using microfluidic networks. Anal Chem 2001;73(6):1240–1246.
101. Kumar A, Whitesides GM. Features of gold having micrometer to centimeter dimensions can be formed through a combination of stamping with an elastomeric stamp and an alkanethiol "ink" followed by chemical etching. Appl Phys Lett 1993;63(14): 2002–2004.
102. Xia Y, Mrksich M, Kim E, Whitesides GM. Microcontact printing of octadecylsiloxane on the surface of silicon dioxide and its application in microfabrication. J Am Chem Soc 1995;117(37):9576–9577.
103. Jeon NL, Finnie K, Branshaw K, Nuzzo RG. Structure and stability of patterned self-assembled films of octadecyltrichlorosilane formed by contact printing. Langmuir 1997;13(13):3382–3391.
104. Xu L, Robert L, Ouyang Q, Taddei Fo, Chen Y, Lindner AB, et al. Microcontact printing of living bacteria arrays with cellular resolution. Nano Lett 2007;7(7):2068–2072.
105. Hidber PC, Nealey PF, Helbig W, Whitesides GM. New strategy for controlling the size and shape of metallic features formed by electroless deposition of copper: microcontact printing of catalysts on oriented polymers, followed by thermal shrinkage. Langmuir 1996;12(21):5209–5215.
106. Perl A, Reinhoudt DN, Huskens J. Microcontact printing: limitations and achievements. Adv Mater 2009;21(22):2257–2268.
107. Kaufmann T, Ravoo BJ. Stamps, inks and substrates: polymers in microcontact printing. Polymer Chem 2010;1(4):371–387.
108. Quist AP, Pavlovic E, Oscarsson S. Recent advances in microcontact printing. Anal Bioanal Chem 2005;381(3):591–600.
109. Kane RS, Takayama S, Ostuni E, Ingber DE, Whitesides GM. Patterning proteins and cells using soft lithography. Biomaterials 1999;20(23–24):2363–2376.
110. Renault JP, Bernard A, Bietsch A, Michel B, Bosshard HR, Delamarche E, et al. Fabricating arrays of single protein molecules on glass using microcontact printing. J Phys Chem B 2003;107(3):703–711.
111. Wilbur JL, Kim E, Xia Y, Whitesides GM. Lithographic molding: a convenient route to structures with sub-micrometer dimensions. Adv Mater 1995;7(7):649–652.
112. von Philipsborn AC, Lang S, Bernard A, Loeschinger J, David C, Lehnert D, et al. Microcontact printing of axon guidance molecules for generation of graded patterns. Nat Protocols 2006;1(3):1322–1328.
113. Murugan R, Ramakrishna S. Design strategies of tissue engineering scaffolds with controlled fiber orientation. Tissue Eng 2007;13(8):1845–1866.
114. Li W-J, Danielson KG, Alexander PG, Tuan RS. Biological response of chondrocytes cultured in three-dimensional nanofibrous poly(ε-caprolactone) scaffolds. J Biomed Mater Res Part A 2003;67A(4):1105–1114.

115. Sell S, Barnes C, Smith M, McClure M, Madurantakam P, Grant J, et al. Extracellular matrix regenerated: tissue engineering via electrospun biomimetic nanofibers. Polymer Int 2007;56(11):1349–1360.

116. Lee CH, Shin HJ, Cho IH, Kang Y-M, Kim IA, Park K-D, et al. Nanofiber alignment and direction of mechanical strain affect the ECM production of human ACL fibroblast. Biomaterials 2005;26(11):1261–1270.

117. Baker BM, Mauck RL. The effect of nanofiber alignment on the maturation of engineered meniscus constructs. Biomaterials 2007;28(11):1967–1977.

118. Agarwal S, Wendorff JH, Greiner A. Progress in the field of electrospinning for tissue engineering applications. Adv Mater 2009;21(32–33):3343–3351.

119. Liao S, Murugan R, Chan CK, Ramakrishna S. Processing nanoengineered scaffolds through electrospinning and mineralization suitable for biomimetic bone tissue engineering. J Mech Behav Biomed Mater 2008;1(3):252–260.

120. Chan CK, Kumar TSS, Liao S, Murugan R, Ngiam M, Ramakrishnan S. Biomimetic nanocomposites for bone graft applications. Nanomedicine 2006;1(2):177–188.

121. Cui W, Zhou Y, Chang J. Electrospun nanofibrous materials for tissue engineering and drug delivery. Sci Technol Adv Mater 2010;11(1):014108.

122. Yang F, Murugan R, Wang S, Ramakrishna S. Electrospinning of nano/micro scale poly (L-lactic acid) aligned fibers and their potential in neural tissue engineering. Biomaterials 2005;26(15):2603–2610.

123. Shi J, Wang L, Zhang F, Li H, Lei L, Liu L, et al. Incorporating protein gradient into electrospun nanofibers as scaffolds for tissue engineering. ACS Appl Mater Interfaces 2010;2(4):1025–1030.

124. Xie J, Li X, Lipner J, Manning CN, Schwartz AG, Thomopoulos S, et al. "Aligned-to-random" nanofiber scaffolds for mimicking the structure of the tendon-to-bone insertion site. Nanoscale 2010;2(6):923–926.

125. Bhaskar S, Lahann J. Microstructured materials based on multicompartmental fibers. J Am Chem Soc 2009;131(19):6650–6651.

126. Bhaskar S, Hitt J, Chang S-WL, Lahann J. Multicompartmental microcylinders. Angew Chem Int Ed 2009;48(25):4589–4593.

127. George MC, Braun PV. Multicompartmental materials by electrohydrodynamic cojetting. Angew Chem Int Ed 2009;48(46):8606–8609.

128. Truskett VN, Watts MPC. Trends in imprint lithography for biological applications. Trends Biotechnol 2006;24(7):312–317.

129. Austin MD, Ge H, Wu W, Li M, Yu Z, Wasserman D, et al. Fabrication of 5 nm linewidth and 14 nm pitch features by nanoimprint lithography. Appl Phys Lett 2004;84(26):5299–5301.

130. Cao H, Tegenfeldt JO, Austin RH, Chou SY. Gradient nanostructures for interfacing microfluidics and nanofluidics. Appl Phys Lett 2002;81(16):3058–3060.

131. Sun JD Y, Lin NJ, Ro HW, Soles CL, Lin-Gibson S. Monitoring alignment of osteoblast cells directed by gradient nanopatterns. In: American Chemical Society 235th National Meeting. New Orleans, 2008.

132. Sun J, Ding Y, Lin NJ, Cicerone MT, Soles CL, Lin-Gibson S. Monitoring of elongation and orientation of osteoblast cells directed by anisotropic nanopatterns. In: Polymer Preprints. Salt Lake City, UT: American Chemical Society; 2009.

133. Mohebi MM, Evans JRG. A drop-on-demand ink-jet printer for combinatorial libraries and functionally graded ceramics. J Comb Chem 2002;4(4):267–274.

134. Sirringhaus H, Kawase T, Friend RH, Shimoda T, Inbasekaran M, Wu W, et al. High-resolution inkjet printing of all-polymer transistor circuits. Science 2000;290(5499): 2123–2126.

135. Pardo L, Wilson WC, Boland T. Characterization of patterned self-assembled monolayers and protein arrays generated by the ink-jet method. Langmuir 2002;19(5): 1462–1466.

136. Okamoto T, Suzuki T, Yamamoto N. Microarray fabrication with covalent attachment of DNA using Bubble Jet technology. Nat Biotech 2000;18(4):438–441.

137. Roth EA, Xu T, Das M, Gregory C, Hickman JJ, Boland T. Inkjet printing for high-throughput cell patterning. Biomaterials 2004;25(17):3707–3715.

138. Xu T, Jin J, Gregory C, Hickman JJ, Boland T. Inkjet printing of viable mammalian cells. Biomaterials 2005;26(1):93–99.

139. Mironov V, Visconti RP, Kasyanov V, Forgacs G, Drake CJ, Markwald RR. Organ printing: tissue spheroids as building blocks. Biomaterials 2009;30(12):2164–2174.

140. Boland T, Xu T, Damon B, Cui X. Application of inkjet printing to tissue engineering. Biotechnol J 2006;1(9):910–917.

141. Nakamura M, Kobayashi A, Takagi F, Watanabe A, Hiruma Y, Ohuchi K, et al. Biocompatible inkjet printing technique for designed seeding of individual living cells. Tissue Eng 2005;11(11–12):1658–1666.

142. Campbell PG, Miller ED, Fisher GW, Walker LM, Weiss LE. Engineered spatial patterns of FGF-2 immobilized on fibrin direct cell organization. Biomaterials 2005;26(33): 6762–6770.

143. Xu T, Petridou S, Lee EH, Roth EA, Vyavahare NR, Hickman JJ, et al. Construction of high-density bacterial colony arrays and patterns by the ink-jet method. Biotechnol Bioeng 2004;85(1):29–33.

144. Alberto D. Exponential gradient maker using a disposable syringe. Anal Biochem 1990;189(1):88–90.

145. Chatterjee K, Lin-Gibson S, Wallace WE, Parekh SH, Lee YJ, Cicerone MT, et al. The effect of 3D hydrogel scaffold modulus on osteoblast differentiation and mineralization revealed by combinatorial screening. Biomaterials 2010;31(19):5051–5062.